JGR Biogeosciences

RESEARCH ARTICLE
10.1029/2021JG006277

Special Section:
Winter limnology in a changing world

# Winter Climate and Lake Morphology Control Ice Phenology and Under-Ice Temperature and Oxygen Regimes in Mountain Lakes

**Adrianne P. Smits[1], Nicholas W. Gomez[1], Jeff Dozier[2], and Steven Sadro[1]**

[1]Department of Environmental Science and Policy, University of California Davis, Davis, CA, USA, [2]Bren School of Environmental Science and Management, University of California Santa Barbara, Santa Barbara, CA, USA

**Key Points:**

- Winter air temperature and snowfall drive ice-off timing and ice phenology of temperate mountain lakes
- Lake size and morphology mediate how climate affects water temperature and dissolved oxygen dynamics during early and late winter
- Rates of hypolimnetic oxygen decline are highest in shallow lakes and do not vary with water temperature

**Supporting Information:**

Supporting Information may be found in the online version of this article.

**Correspondence to:**

A. P. Smits,
adriannesmits@gmail.com

**Citation:**

Smits, A. P., Gomez, N. W., Dozier, J., & Sadro, S. (2021). Winter climate and lake morphology control ice phenology and under-ice temperature and oxygen regimes in mountain lakes. *Journal of Geophysical Research: Biogeosciences*, *126*, e2021JG006277. https://doi.org/10.1029/2021JG006277

Received 1 FEB 2021
Accepted 26 JUL 2021

**Author Contributions:**

**Conceptualization:** Adrianne P. Smits, Steven Sadro
**Data curation:** Adrianne P. Smits, Nicholas W. Gomez, Jeff Dozier
**Formal analysis:** Adrianne P. Smits, Jeff Dozier
**Funding acquisition:** Adrianne P. Smits
**Investigation:** Nicholas W. Gomez
**Methodology:** Nicholas W. Gomez
**Visualization:** Adrianne P. Smits, Steven Sadro



**Abstract** Warming winters will reduce ice cover and change under-ice conditions in temperate mountain lakes, where snow contributes most of winter cover on lakes. Snow-dominated mountain lakes are abundant and highly susceptible to climate warming, yet we lack an understanding of how climate variation and local attributes influence winter processes. We investigated climatic and intrinsic controls on ice phenology, water temperature, and bottom-water dissolved oxygen (DO) in 15 morphologically diverse lakes in the Sierra Nevada and Klamath Mountains of California, USA, using high-frequency measurements from multiple (2–5) winters. We found that ice phenology was determined by winter climate variables (snowfall and air temperature) that influence ice-off timing, whereas ice-on timing was relatively invariant among years. Lake size and morphology mediated the effect of climate on lake temperature and DO dynamics in early and late winter. Rates of hypolimnetic DO decline were highest in small, shallow lakes, and were unrelated to water temperature. Temperature and oxygen dynamics were more variable in small lakes because heavy snowfall caused ice submergence, mixing, and DO replenishment that affected the entire water column. As the persistence of snow declines in temperate mountain regions, autumn, and spring climatic conditions are expected to gain importance in regulating lake ice phenology. Water temperature and DO will likely increase in most lakes during winter as snowpack declines, but morphological attributes such as lake size will determine the sensitivity of ice phenology and under-ice processes to climate change.

**Plain Language Summary** Mountain lakes in temperate regions are at risk of losing ice cover as winters become warmer and snowfall decreases. Small mountain lakes are numerous and provide important habitats for aquatic species, yet we currently lack an understanding of what controls ice duration and under-ice conditions in these snow-dominated systems because most are remote and inaccessible. We used hourly measurements within a diverse set of California mountain lakes across multiple winters to explore how climate variables and lake or watershed characteristics influence the duration and timing of ice cover, as well as under-ice temperature and oxygen concentrations. We found that winter snowfall and air temperature controlled the timing of ice breakup and the length of ice duration. Lake size and shape controlled oxygen and temperature immediately after ice formation, but late winter conditions depended on winter climate variables that dictated ice cover duration. Oxygen depletion rates and the prevalence of low oxygen conditions were greater in small, shallow lakes than in large, deep lakes. As winters warm, most mountain lakes will have shorter ice cover, warmer water temperatures, and increased oxygen concentrations, but small and large lakes will respond differently to the loss of snow and ice cover.

## 1. Introduction

Ice cover is decreasing in many of the world's lakes (Sharma et al., 2019), creating an urgent need to understand drivers of ice phenology and winter ecology in a diversity of lake types (Hampton et al., 2017; Warne et al., 2020). Ice cover duration and timing affect ecosystem functions during open water seasons, such as thermal and mixing regimes (Smits et al., 2020; Woolway et al., 2020), oxygen dynamics (Flaim et al., 2020), and primary productivity (Hampton et al., 2017; Sadro et al., 2018b). Ice cover directly controls winter processes such as under-ice thermal stratification and circulation (Kirillin et al., 2012), oxygen depletion (Granados et al., 2020; Leppi et al., 2016; Obertegger et al., 2017), carbon and nutrient cycling (Denfeld

**Writing – original draft:** Adrianne P. Smits
**Writing – review & editing:** Adrianne P. Smits, Nicholas W. Gomez, Jeff Dozier, Steven Sadro

et al., 2018; Powers et al., 2017; Rue et al., 2020), and phytoplankton productivity (Maier et al., 2019). Primary productivity under the ice can make up a significant fraction of total annual productivity in many lakes (Hampton et al., 2017), and dissolved oxygen (DO) dynamics beneath the ice dictate the amount and distribution of suitable habitat for aquatic organisms such as fishes (Stefan et al., 2001). All these processes are likely to change as lakes lose ice cover, yet winter limnology lags behind our understanding of open-water seasons and is often focused on cross-seasonal linkages rather than on dynamics under ice (Hampton et al., 2017).

Small lakes dominate the global distribution (<1 $km^2$ surface area; Downing et al., 2006), and midlatitude lakes are at greatest risk of ice loss as air temperature rises (Sharma et al., 2019), but climate change impacts on ice cover have been monitored mostly in large lakes at high latitudes (Magnuson et al., 2000; Sharma et al., 2019). Lakes that develop seasonal ice cover despite moderate winter air temperatures, such as mountain lakes in the western US, may be subject to declining trends in ice cover and shifts in associated processes (Caldwell et al., 2020; Sadro et al., 2018a), yet they remain under-studied due to their inaccessibility and small size. Mountain landscapes contain heterogeneous topography and microclimates that mediate the expression of climate forcing (Novikmec et al., 2013; Sadro et al., 2018a), complicating efforts to predict lake responses at regional scales in these systems. Strong linkages between winter climate, ice phenology, and summer thermal or chemical conditions in temperate mountain lakes have been demonstrated (Oleksy et al., 2020; Preston et al., 2016; Sadro et al., 2018a; Smits et al., 2020). However, drivers of winter processes in small mountain lakes remain essentially unexplored—few studies of under-ice processes have been attempted (e.g., Granados et al., 2020).

The classic concepts of "Winter I" and "Winter II" formulated by Kirillin et al. (2012) provide a framework for understanding physical dynamics in lakes that experience snow and ice cover. During Winter I, snow covers lake ice, blocking light transmission, and circulation is driven by gravity currents and heat release from sediments. During Winter II, snow atop the ice melts and the remaining clear ice allows radiation-driven convective mixing and photosynthesis by phytoplankton, depending on the overlap between the mixed layer and photic depth (Pernica et al., 2017). However, the applicability of these concepts to lakes remains untested in warmer regions with a substantial winter snowpack, where lake "ice" is often comprised of layered snow-ice lenses rather than clear ice covered by snow (Block et al., 2019; Leppäranta, 2015), and can be several meters thick. In mid-latitude mountain ranges snowfall varies considerably among years, generating large inter-annual differences in lake ice thickness and under-ice conditions (Granados et al., 2020; Smits et al., 2020). A heavy snowpack melts later, delays ice-off (Caldwell et al., 2020; Preston et al., 2016; Sadro et al., 2018a), and is associated with greater oxygen depletion under ice (Granados et al., 2020; Obertegger et al., 2017). However, general understanding of winter limnology in snow-dominated mountain lakes, including drivers of temporal and spatial variation, is lacking.

Mountain lakes are experiencing rapid changes owing to climatic trends (Pepin et al., 2015; Sadro et al., 2018a), including more frequent snow droughts and mid-winter rain events as air temperatures increase (Dettinger et al., 2015; Harpold et al., 2017). Changes in the magnitude, timing, and form of precipitation will alter the snowpack, lake ice cover, and under-ice thermal and chemical processes. However, lake size and morphology and catchment topography should mediate the effects of climate variation on ice phenology and associated processes (Arp et al., 2013; Leppi et al., 2016; Novikmec et al., 2013). This study explores the roles of inter-annual climate variation and lake and watershed characteristics in determining ice phenology and under-ice physical and chemical conditions in lakes with snow-dominated catchments.

We investigated climatic and intrinsic (lake or watershed-specific) controls on ice phenology, water temperature, and bottom-water DO in 15 lakes in the Sierra Nevada and Klamath Mountains of California, USA, using hourly measurements from two contrasting winters (2019–2020; high snow and low snow). We also quantified inter-annual variation in lake ice phenology and under-ice conditions in a small high-elevation lake with five winters of measurements (Emerald Lake; water years 2016–2020). The studied lakes span elevations from 1,500 to 3,500 m and vary considerably in size and morphology, allowing comparison of the relative importance of climate variation (precipitation, air temperature, and shortwave radiation) versus intrinsic factors (size, morphology, and watershed characteristics). We asked the following questions: (a) How does inter-annual variation in temperature and precipitation affect ice phenology and under-ice conditions? and (b) How do watershed or lake characteristics mediate lake responses to climate variation? We aimed

to understand which winter processes are most sensitive to warming temperatures and decreased snowfall, and whether climate sensitivity varies among lakes.

## 2. Materials and Methods

### 2.1. Site Description and Overview

The 15 study lakes in the Sierra Nevada and Klamath Mountains of California, USA (Figure 1a) spanned substantial ranges (Table 1) in elevation (1,554–3,559 m.a.s.l.), surface area (2–60 ha), and depth (maximum depth 6–80 m). The study lakes are located in small watersheds (1.1–4.5 $km^2$) of primarily granitic bedrock, and their small range in surface areas is typical of the lake size distribution in the Sierra Nevada mountains (95% of lakes < 15 ha; Melack et al., 2021). There was no correlation between surface area and elevation ($r = 0.12$) of the study lakes. All lakes except Swamp developed ice cover each year and received most of their annual precipitation as snow. Hourly sensor measurements were obtained from all 15 lakes in water years 2019 and 2020 (WY, which corresponds to October 1 in the previous calendar year through September 30 in the current calendar year). At Emerald Lake, a small, high elevation lake in Sequoia National Park that has been a long-term study site for decades (Figures 1b and 1c; Melack et al., 2021), we made hourly measurements in three more water years (2016–2020).

### 2.2. High-Frequency Lake Measurements

We installed a vertical sub-surface array of thermistors (Onset Hobo Water Temperature Pro v2, accuracy ±0.2°C, resolution ±0.02°C) at or near the deepest point in each lake to record hourly water temperature year-round (0.5–8 m vertical spacing, 5–20 thermistors per lake; Table 1). Thermistor arrays were retrieved once each year during the open water season (May– October) to replace instruments and then redeployed in the same location. The top-most thermistor on each array was situated approximately 3 m below the lake surface to avoid entrainment in lake ice during winter. A thermistor attached to the bottom of each array recorded sediment temperature 5–10 cm below the sediment-water interface, except in the two deepest lakes, Dorothy and Ireland. A sub-surface light sensor (Onset Hobo Pendant) was attached to the top of each array to record relative light intensity to verify ice-on and ice-off dates and to capture periods of ice-thinning. A DO sensor (PME MiniDOT; resolution ±0.3 mg $L^{-1}$) and specific conductance (SC) sensor (Onset U24; ±5 μS $cm^{-1}$) were installed within 2 m of the lake bottom on each array and recorded data hourly. Emerald Lake, a long-term study site, had a similar array installation as the other study lakes, but 3–4 sensors were added during each summer to capture thermal dynamics within the top 3 m of the water column. In the summer of calendar year 2017, thermistors in Emerald Lake were replaced with RBR sensors (SoloT; accuracy ±0.002°C, resolution <0.00005°C). All instruments were inter-calibrated and corrected for temperature using a shared water bath. DO sensor calibration was evaluated pre-deployment and post-deployment in 0% and 100% solutions and corrected for offset or drift as necessary.

### 2.3. Determining Ice Phenology

We estimated dates of ice-formation and ice-breakup from high-frequency time series of temperature, DO, and light intensity, following recommendations in Pierson et al. (2011). Ice-on dates were initially determined as the onset of inverse stratification in autumn between the top and bottom-most temperature sensor in each lake (difference exceeding 0.1°C), and then verified by visual inspection of light intensity time series (e.g., abrupt reduction in light; Figures S2 and S3). Ice-off dates were determined from increases in light intensity and DO rather than from the onset of isothermal conditions in spring, as snowmelt intrusions beneath ice-cover caused some smaller lakes (e.g., Emerald Lake) to mix before ice-off. At Emerald Lake, sensor-based ice-off dates were verified using daily images from a game camera mounted on-shore.

### 2.4. Climate Data

We used down-scaled climate variables acquired from the GRIDMET data set for each lake and all water years (2016–2020) to explore climatic controls on ice phenology and lake conditions, following methods used in Caldwell et al. (2020). GRIDMET (Abatzoglou, 2013), a gridded surface meteorological data

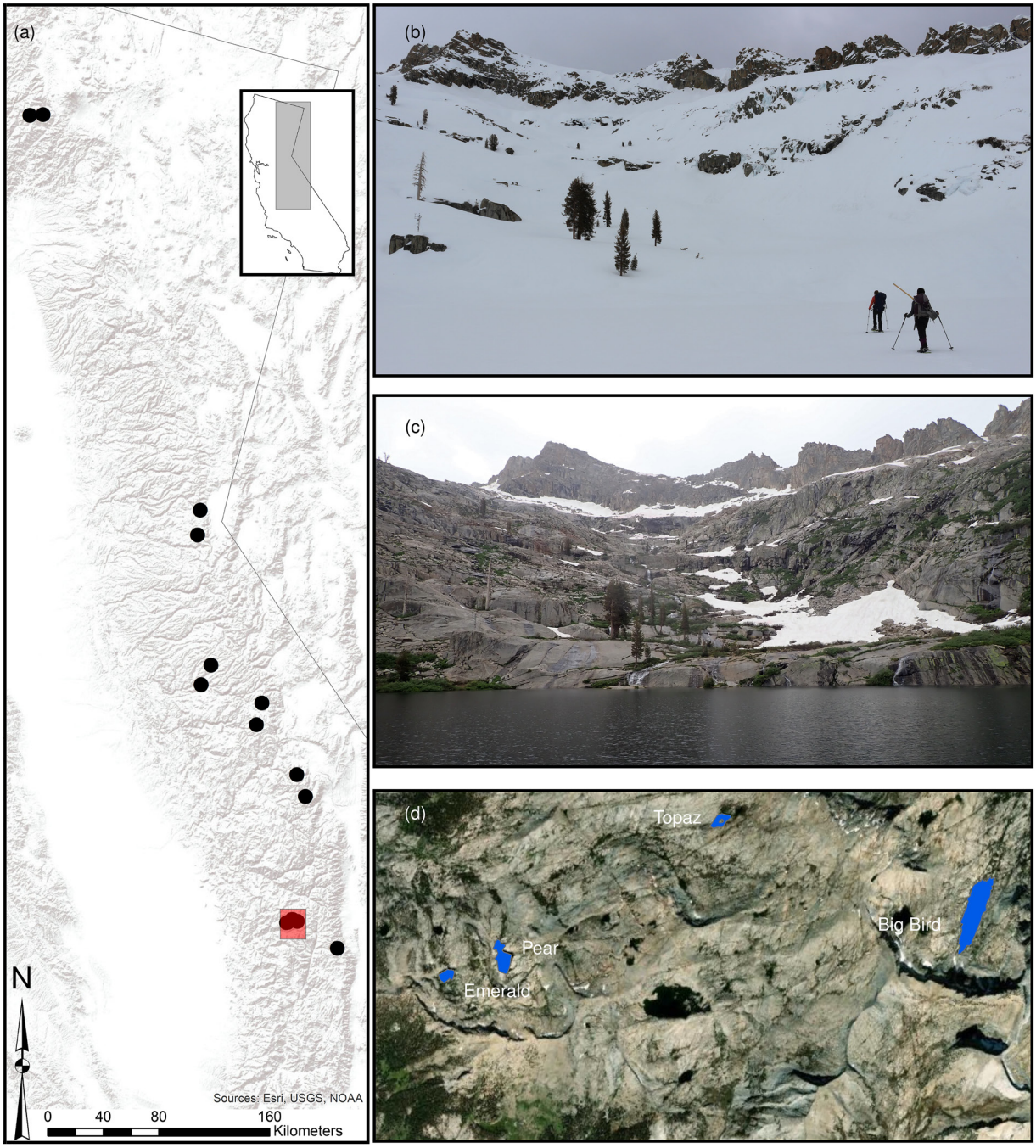


**Figure 1.** (a) Study lakes (black dots) located in the Sierra Nevada and Klamath Mountains of California, USA (inset shows geographic extent). (b) Deep snow covers ice on Emerald Lake (2,800 m.a.s.l.) in April 2019. (c) Emerald Lake, ice-free, in July 2019. (d) Four lakes (blue polygons; Emerald, Pear, Topaz, Big Bird) located within 10 km distance in Sequoia National Park (red rectangle in panel (a)) that vary in size and morphology.

set for the continental United States with 4 × 4 km$^2$ spatial resolution and daily temporal resolution, has been previously used to explore effects on snow in western US mountains (Abatzoglou, 2013; Harpold & Brooks, 2018). We downloaded daily values of mean and minimum air temperatures (°C), total precipitation (mm), and mean shortwave radiation (W m$^{-2}$). We calculated daily total precipitation falling as snow (snowfall; mm) using a temperature-based regression model (Dingman, 2002), as follows: if air temperature was below 0°C, snowfall is equivalent to the total precipitation. If air temperature was between 0 and 6°C, then snowfall = total precipitation – 0.1678*air temperature. Given the coarse spatial and temporal

**Table 1**
*Study Site Attributes, Including the Number of Temperature Sensors Deployed in Each Lake and Water Year (WY)*

| Lake | WY | Sensors (#) | Latitude (deg.) | Longitude (deg.) | Elevation (m) | Max depth (m) | Mean depth (m) | Lake area ($m^2$) | Volume ($m^3$) | Littoral area (%) | Shading (% day) | Watershed area ($km^2$) |
|---|---|---|---|---|---|---|---|---|---|---|---|---|
| Swamp | 2019; 2020 | 8; 8 | 37.9500 | −119.8290 | 1,554 | 19.4 | 11.4 | $6.85 \times 10^4$ | $7.78 \times 10^5$ | 17 | 19 | 1.65 |
| Castle | 2019; 2020 | 8; 12 | 41.2271 | −122.3834 | 1,646 | 34.5 | 10.3 | $2.02 \times 10^5$ | $2.08 \times 10^6$ | 36 | 30 | 1.36 |
| Cliff | 2019; 2020 | 8; 8 | 41.1991 | −122.4908 | 1,760 | 25.6 | 7.6 | $6.71 \times 10^4$ | $6.50 \times 10^5$ | 24 | 47 | 1.42 |
| Miller | 2019; 2020 | 8; 8 | 39.0352 | −120.2001 | 2,175 | 7.5 | 2.8 | $1.21 \times 10^5$ | $3.36 \times 10^5$ | 60 | 9 | 1.33 |
| Boundary | 2019; 2020 | 8; 8 | 38.0886 | −119.7898 | 2,294 | 32.4 | 7.7 | $1.81 \times 10^5$ | $1.79 \times 10^6$ | 26 | 13 | 1.27 |
| Clyde | 2019; 2020 | 8; 8 | 38.8757 | −120.1695 | 2,460 | 10.4 | 5.2 | $8.92 \times 10^4$ | $4.68 \times 10^5$ | 25 | 38 | 1.10 |
| Emerald | 2016–2020 | 20; 19; 13; 14; 13 | 36.5975 | −118.6758 | 2,800 | 9.6 | 5.3 | $2.82 \times 10^4$ | $1.49 \times 10^5$ | 28 | 43 | 1.10 |
| Pear | 2019; 2020 | 15; 14 | 36.6007 | −118.6672 | 2,900 | 23.7 | 6.6 | $7.46 \times 10^4$ | $4.95 \times 10^5$ | 37 | 36 | 1.53 |
| Big Bird | 2019; 2020 | 8; 9 | 36.6216 | −118.5934 | 2,978 | 38.3 | 13.4 | $2.73 \times 10^5$ | $3.86 \times 10^6$ | 19 | 35 | 3.82 |
| Dorothy[a] | 2019; 2020 | 9; 12 | 37.5387 | −118.8825 | 3,135 | 80.8 | 31.3 | $6.14 \times 10^5$ | $2.07 \times 10^7$ | 5 | 23 | 4.02 |
| Skelton[b] | 2019; 2020 | 8; 9 | 37.9322 | −119.3045 | 3,200 | 11 | 5.5 | $5.19 \times 10^4$ | $2.73 \times 10^5$ | 32 | 24 | 2.05 |
| Topaz | 2019; 2020 | 5; 5 | 36.6262 | −118.6372 | 3,219 | 6.5 | 1.5 | $3.87 \times 10^5$ | $5.98 \times 10^4$ | 89 | 7 | 1.32 |
| Ireland | 2019; 2020 | 9; 10 | 37.7888 | −119.3046 | 3,272 | 70.1 | 26.1 | $4.34 \times 10^5$ | $1.27 \times 10^7$ | 12 | 21 | 3.78 |
| Ruby | 2019; 2020 | 8; 8 | 37.4150 | −118.7700 | 3,397 | 32.1 | 15.5 | $1.48 \times 10^5$ | $2.29 \times 10^6$ | 12 | 32 | 4.49 |
| Cottonwood6 | 2019; 2020 | 8; 8 | 36.513 | −118.226 | 3,559 | 12.4 | 6.0 | $2.02 \times 10^4$ | $1.19 \times 10^5$ | 26 | 26 | 1.26 |

*Note*. Littoral area refers to the percentage of a lake's surface area where depth is less than 3 m. Shading (% day) is the annual mean percentage of daylight hours during which surrounding topography shades the lake surface from direct solar illumination.
[a]In Dorothy Lake, the thermistor array was not located at the deepest point during WY 2019 (installed at 63 m depth), but was moved near to the deepest location in WY 2020 (78 m). [b]Skelton Lake thermistor chain was not installed until October of calendar year 2018.

resolution of the climate data set, we calculated seasonal climate metrics (e.g., mean autumn air temperature and total winter snowfall) as explanatory factors for seasonal-scale lake behavior, rather than attributing lake responses to individual weather events at diel or multi-day time scales. From the daily data sets, we calculated climate metrics for autumn (October 1–December 1), winter (December 1–March 1), and spring (March 1–May 1). For autumn, we calculated average daily mean temperature, average daily minimum temperature, total cumulative precipitation, and cumulative daily mean shortwave radiation. For winter and spring, we calculated these same metrics, as well as cumulative snowfall.

For each lake and each day of the year, we calculated the fraction of the daylight periods when topography obscures direct solar illumination at the center of the lake, by computing the angle to the local horizons for all azimuths and comparing those angles to the solar zenith angle and azimuth throughout each day (Dozier & Frew, 1990). We calculated annual and seasonal mean percent shading for each lake (autumn, winter, and spring).

### 2.5. Modeling Seasonal DO Depletion Rates

We estimated bottom-water DO depletion rates (mg $L^{-1}$ $day^{-1}$) during the period of ice cover following the approach described in Obertegger et al. (2017), using the R statistical software (R Core Team, 2015). Hourly DO data were aggregated to daily means before analyzing trends. Before trend estimation, DO time series was split at change points in variance using the "changepoint" package in R (Killick et al., 2016), to avoid biasing subsequent time series analysis (Zeileis et al., 2003). This resulted in 1–3 time series per winter for each lake, depending on the number of change points, which were then analyzed separately for DO trends. DO depletion rates (trends) were estimated by modeling each time series as an autoregressive integrated moving average (ARIMA($p$,$d$,$q$)), where $p$ is the number of autoregressive terms, $d$ is the degree of differencing, and $q$ is the number of previous time-steps contributing to the weighted error term at any given time point. When $d = 1$, the original data are not stationary, but rather show a trend (e.g., DO depletion

rate) that can be estimated. We tested for stationarity (or lack thereof) of DO time series using the Kwiatowski-Phillips-Schmidt-Shin test, and then fit ARIMA models using the "forecast" package in R (Hyndman et al., 2020). Model residuals were tested for heterogeneity using the Ljung-Box test and by examining plots of autocorrelation functions. A higher-order ARIMA($p$,1,$q$) was fitted to the data if model residuals exhibited non-stationarity. All DO trend estimates are reported in Table S2, but only DO trends immediately following ice formation were used in subsequent analyses.

### 2.6. Calculating Lake Thermal Metrics

For each lake-year combination, we calculated metrics of lake thermal conditions before and during ice cover using the "Lake Analyzer" package in R (Read et al., 2011). Before analyses, hourly water temperature data were aggregated to daily means. For each lake year, we calculated daily time series of volume-weighted mean water temperature and summed water column heat content using temperature measurements at multiple depths and lake hypsographic curves. The duration of fall mixing was computed as the period between when the water column became isothermal (<0.2°C between the top and bottom-most temperature sensor in each lake) and ice-on.

### 2.7. Regression Models

To explore intrinsic (lake or watershed-specific) and climatic controls on lake ice phenology and under-ice thermal and chemical conditions, we fitted single-predictor and multiple regression models. Response variables related to under-ice conditions were calculated separately for early winter (W1) and late winter (W2). Because the timing of these periods varied both among lakes within a year and among years, we defined them relative to ice phenology as follows: W1 is defined as the 2 months following ice-on, and W2 is defined as the period from the end of W1 until a month before ice-off.

We used the following response variables: ice-on calendar day of year (DOY), ice-off DOY, ice duration (days), mean whole lake (volume-weighted) water temperature under the ice in early winter (W1) and late winter (W2), DO depletion rate immediately following ice-on (mg $L^{-1}$ $day^{-1}$), and duration of hypoxia under ice (DO < 2 mg $L^{-1}$; days).

Predictors used in regression models included seasonal climate metrics (air temperature, precipitation, snowfall, and shortwave radiation; described in "Climate data" section), dynamic lake thermal or ice cover metrics (e.g., maximum summer water temperature, mean W1 water temperature, and ice-on DOY), as well as intrinsic lake or watershed characteristics related to lake size, lake morphology, and topography. Lake size and morphological variables included maximum lake depth, mean lake depth, lake surface area, lake volume, and percent littoral surface area (percent of lake surface area with depth <3 m). In addition, because lake depths were skewed toward small, shallow lakes, we created two lake depth categories to use in regressions: shallow (maximum depth < 15 m; $n = 6$) and deep (maximum depth > 15 m; $n = 9$). Watershed variables included latitude (°), elevation (m.a.s.l.), mean watershed slope (°), and topographic shading (seasonal or annual means). For ice-on models, we used the mean percentage of daylight hours each lake surface was shaded during autumn (October 1–December 1) as our metric of topographic shading. For ice-off models, we used annual mean shading as well as seasonal values (winter and spring).

We fit linear regression models using maximum likelihood and compared model fits using Akaike's Information Criterion for small sample sizes using the "AICcmodavg" package in R ($AIC_c$; Burnham & Anderson, 2002; Mazerolle, 2020). A difference in $AIC_c$ ($\Delta AIC_c$) greater than 4 between the two models indicates moderate support for the model with lower $AIC_c$, whereas $\Delta AIC_c > 10$ indicates strong support. We compared all regression models to an intercept-only null model—we considered any models within 2 $AIC_c$ units of the null model as insignificant. We first fitted single-predictor models (13–18 candidate models per response variable). Predictors that improved model fits relative to the intercept-only model were then combined in multiple regression models, with a maximum of 3 predictors per model. If predictors were highly correlated ($r > 0.7$; see Table S3 for full correlation matrix between predictor variables), we included only the predictor with the strongest relationship to the response variable in multiple regression models. Due to our relatively small sample size, we allowed only additive effects in the multiple regression models and compared model fits to the single-predictor models and the intercept-only models.

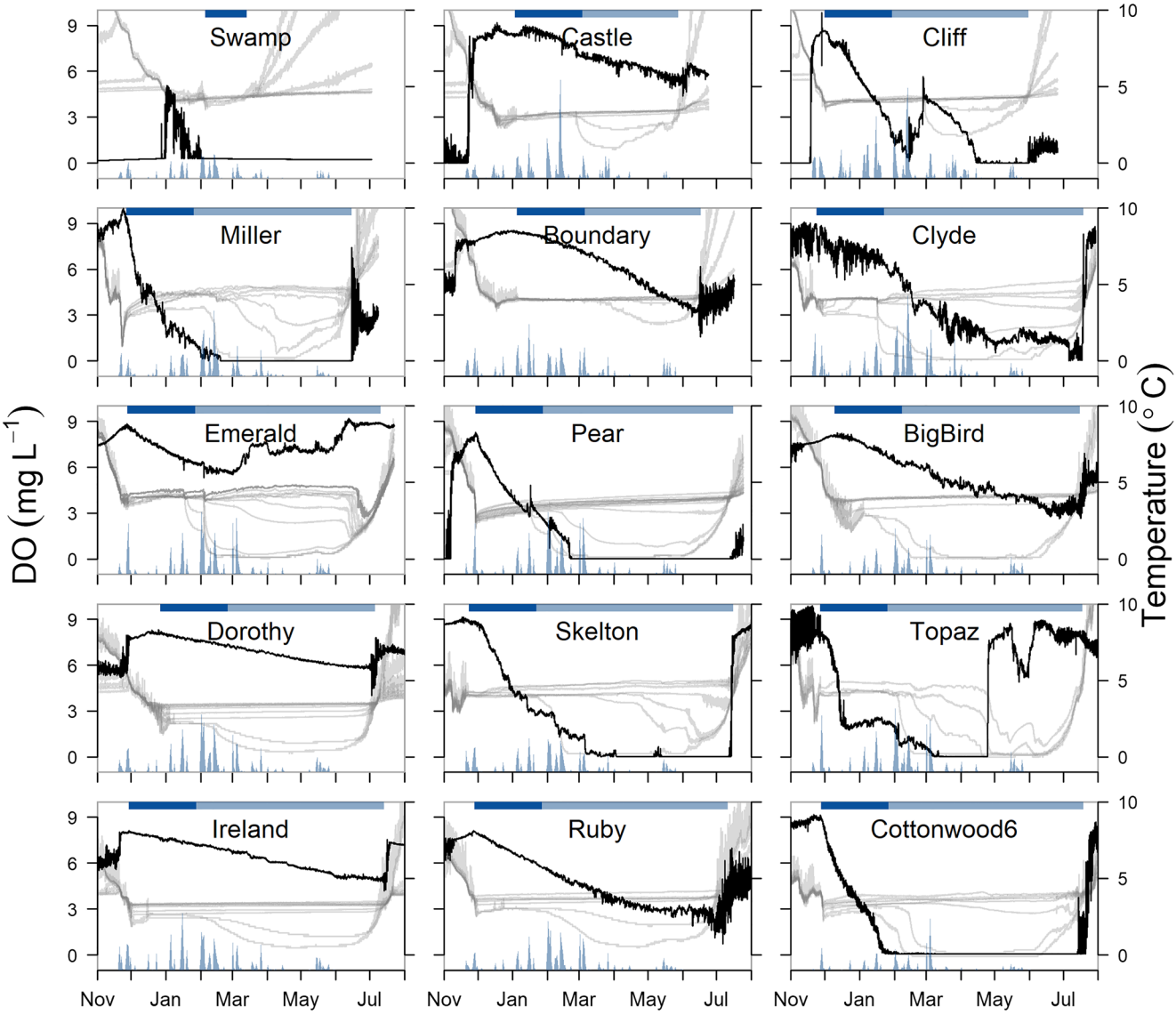


**Figure 2.** Ice duration and under-ice thermal and chemical conditions in WY 2019 (*x*-axis from November 1, 2018 to August 1, 2019). Panels are ordered by increasing elevation (left to right and top to bottom). Black solid lines represent hourly DO concentration (left *y*-axis; mg $L^{-1}$) within 3 m of the lake bottom, at or near the deepest point in each lake. Gray solid lines represent hourly water temperature (right *y*-axis; °C) at discrete depths from the lake bottom to approximately 3 m beneath the surface. Blue bars at the top of each panel represent the longest continuous ice-covered period for each lake. The dark blue portion of bar shows the time period corresponding to W1. Light blue filled time series at the bottom of each panel show mean daily snowfall (mm; plotting range 0–300 mm). Time series from thermistor chains that were retrieved and downloaded before August 1 appear truncated.

## 3. Results

### 3.1. Climatic Conditions

Climatic conditions differed substantially between WY 2019 and 2020 (Figure S1), and consequently lake ice phenology and under-ice conditions also differed (Figures 2 and 3, Table S1; Smits, 2021). Across all sites, mean autumn air temperatures were similar in WY's 2019 and 2020 (3.36 vs. 3.20°C; $p > 0.1$), although roughly twice as much total precipitation fell in autumn of WY 2019 (mean among sites: 230 mm) compared with 2020 (115 mm; $p < 0.001$). Winter of WY 2019 was both colder and wetter than WY 2020. Winter air temperatures were lower in WY 2019 than in WY 2020 (−3.35 vs. −1.89°C; $p < 0.1$), and almost 3 times more snow fell (average total snowfall 849 vs. 290 mm; $p < 0.001$; Figure S1). The seasonal distribution of snowfall diverged between the 2 years: early winter precipitation was similar, but much of the total snowfall in 2019

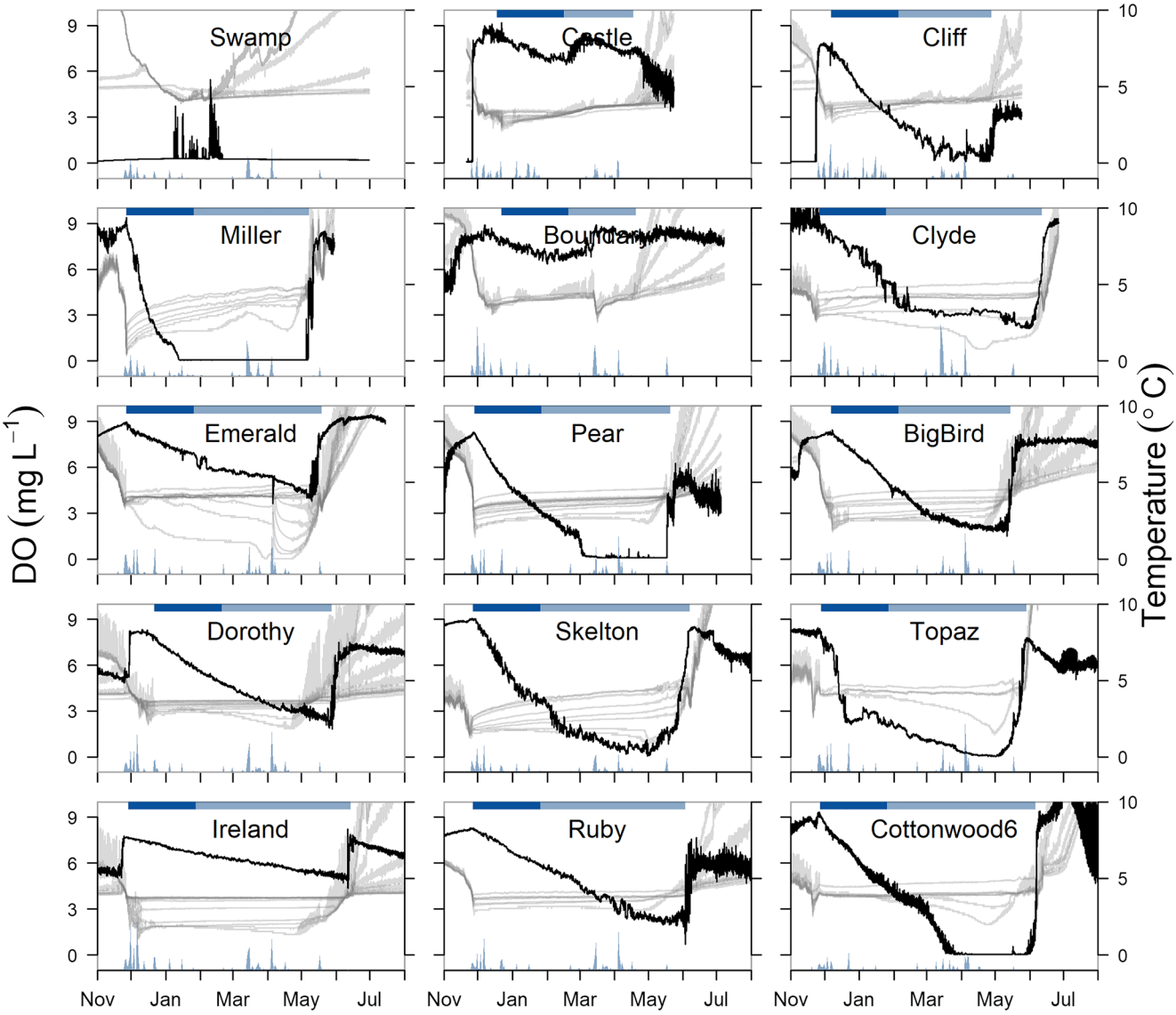


**Figure 3.** Ice duration and under-ice thermal and chemical conditions in WY 2020 (*x*-axis extent from November 1, 2019 to August 1, 2020). Symbols are as in Figure 2.

fell in January and February, whereas in 2020, January and February lacked substantial snowfall (Figures 2 and 3; blue time series).

### 3.2. Summer Lake Temperature and Autumn Mixing

Small, shallow lakes (<15 m maximum depth) attained higher maximum temperatures during the summer than deeper lakes (17.17 vs. 11.25°C; $p < 0.001$). For lakes that stratified, the duration of fall mixing lasted from less than a week to over 2 months, with larger variation among smaller lakes (Table S1; Smits, 2021). Lakes with large surface areas tended to have a shorter mixing duration than smaller lakes. Four small, shallow high-elevation lakes (Topaz, Cottonwood 6, Clyde, Skelton; maximum depth < 13 m, >2,400 m.a.s.l.) were polymictic in at least one summer and thus lacked a distinct fall mixing period.

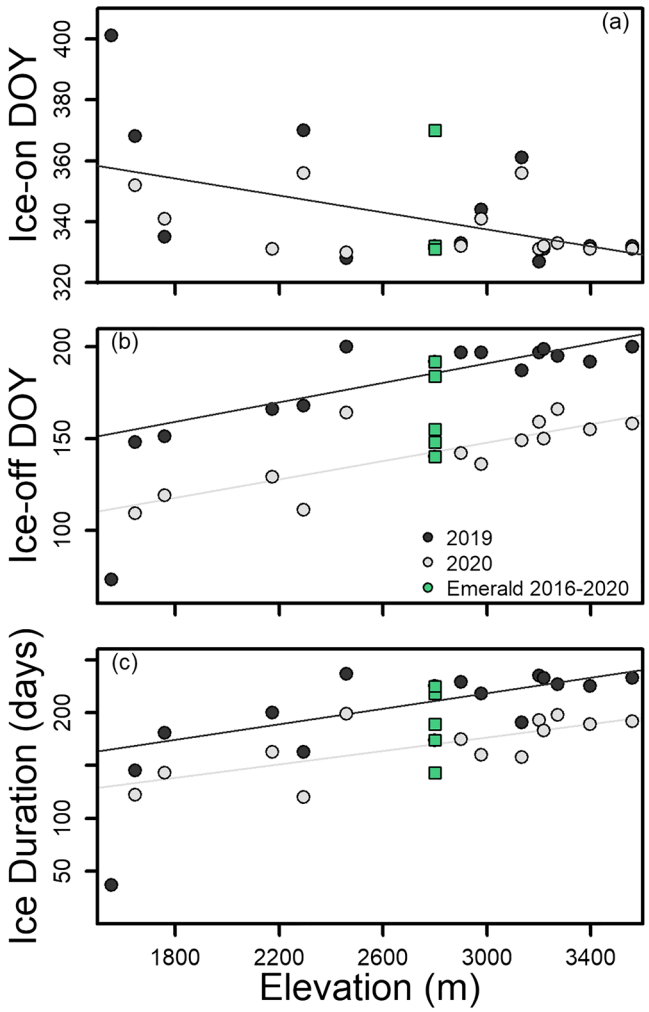


**Figure 4.** Changes in (a) ice-on DOY, (b) ice-off DOY, and (c) ice duration with elevation for all study lakes and study years. Lines show regression relationships between elevation and ice-on DOY, ice-off DOY, and ice duration. In panels (b and c), separate regression lines for WY 2019 (black) and WY 2020 (gray) are shown. Green squares represent WY 2016–2020 in Emerald Lake.

### 3.3. Ice Phenology

Ice phenology responded more directly to variation in winter climate than to autumn climate in the 2 study years. The large snowpack in WY 2019 extended ice-off in most lakes, and thus also ice duration. Excluding Swamp lake, which did not develop ice cover in WY 2020, ice-on dates were similar in both years (average: December 5 vs. December 3; $p > 0.1$, ANCOVA with elevation, Figure 4a), whereas ice-off dates were over a month later in 2019 than in 2020 (July 3 vs. May 21; $p < 0.01$, ANCOVA with elevation, Figure 4b). Later ice-off dates in 2019 resulted in approximately 40 additional days of ice cover ($p < 0.01$, ANCOVA with elevation; Figure 4c).

Different seasonal distribution of snowfall between the two winters generated distinct temporal patterns in snow and ice cover thickness and light transmissivity, especially in low-elevation and larger lakes. In 2019, abundant mid-winter snowfall generated a thick ice and snow cover on most lakes that blocked light transmission until the onset of spring snowmelt (Figures 2 and S2). In contrast, the lack of mid-winter snowfall in 2020 allowed ice and snow cover to thin and water temperature and DO to increase in several low-elevation lakes (Castle, Cliff, and Boundary lakes; Figure 3). Large lakes at higher elevations, such as Big Bird and Dorothy, also experienced mid-winter ice thinning in WY 2020, as evidenced by increases in sub-surface light intensity (Figure S3).

### 3.4. Under-Ice Thermal and Chemical Conditions

Under-ice water temperature was more variable in the wetter winter (WY 2019) than in WY 2020, driven by the behavior of small, shallow lakes (Figures 5a and 5b; purple time series). In both years, shallow lakes showed greater increases in volume-weighted mean water temperature than larger lakes following ice-on (Figures 5a and 5b), as well as greater decreases in temperature in late winter and during spring snowmelt. In both years, volume-weighted mean water temperature increased in most lakes during W1 and decreased during W2. In WY 2019, lakes were slightly but not significantly warmer in early winter than in 2020 ($3.55 \pm 0.50$ vs. $3.31 \pm 0.61$°C; $p > 0.1$), but by late winter water temperatures were lower in 2019 than in 2020 ($2.90 \pm 0.65$ vs. $3.46 \pm 0.42$°C; $p < 0.05$).

Winter snowfall often coincided with decreasing water temperature in the upper water column (Figure 2). Temperature declines following snowstorms affected a larger portion of the water column in shallow lakes, leading to more dynamic thermal behavior overall. SC of bottom waters was generally low in all lakes ($9.95 \pm 4.27$ µS cm$^{-1}$; Figures 5c and 5d), but shallow lakes occasionally showed large increases during spring snowmelt, especially in WY 2019 (Figure 5c).

### 3.5. Dissolved Oxygen Under Ice

Bottom water DO depletion rates were fastest immediately after ice-on and were similar in both years ($-0.07 \pm 0.07$ mg L$^{-1}$ day$^{-1}$; range $-0.0001$ to $0.322$ mg L$^{-1}$ day$^{-1}$; $p > 0.1$). Rates of DO decline slowed or ceased during late winter in shallow lakes but remained relatively constant in the deepest lakes (Ireland and Dorothy) throughout the ice-covered period, with fewer significant change points in the DO time series (Figures 2, 3, 5e, and 5f; Table S2). Initial rates of DO depletion were greatest in shallow lakes regardless of elevation (Figures 5e, 5f, and 7a). DO often increased before ice-off in shallow lakes without any concurrent increases in sub-surface light (Figures 2, 3, S2, and S3), causing late winter DO to vary more in shallow lakes than in deep lakes (Figures 5e and 5f). Most study lakes developed hypoxic bottom waters in both years,

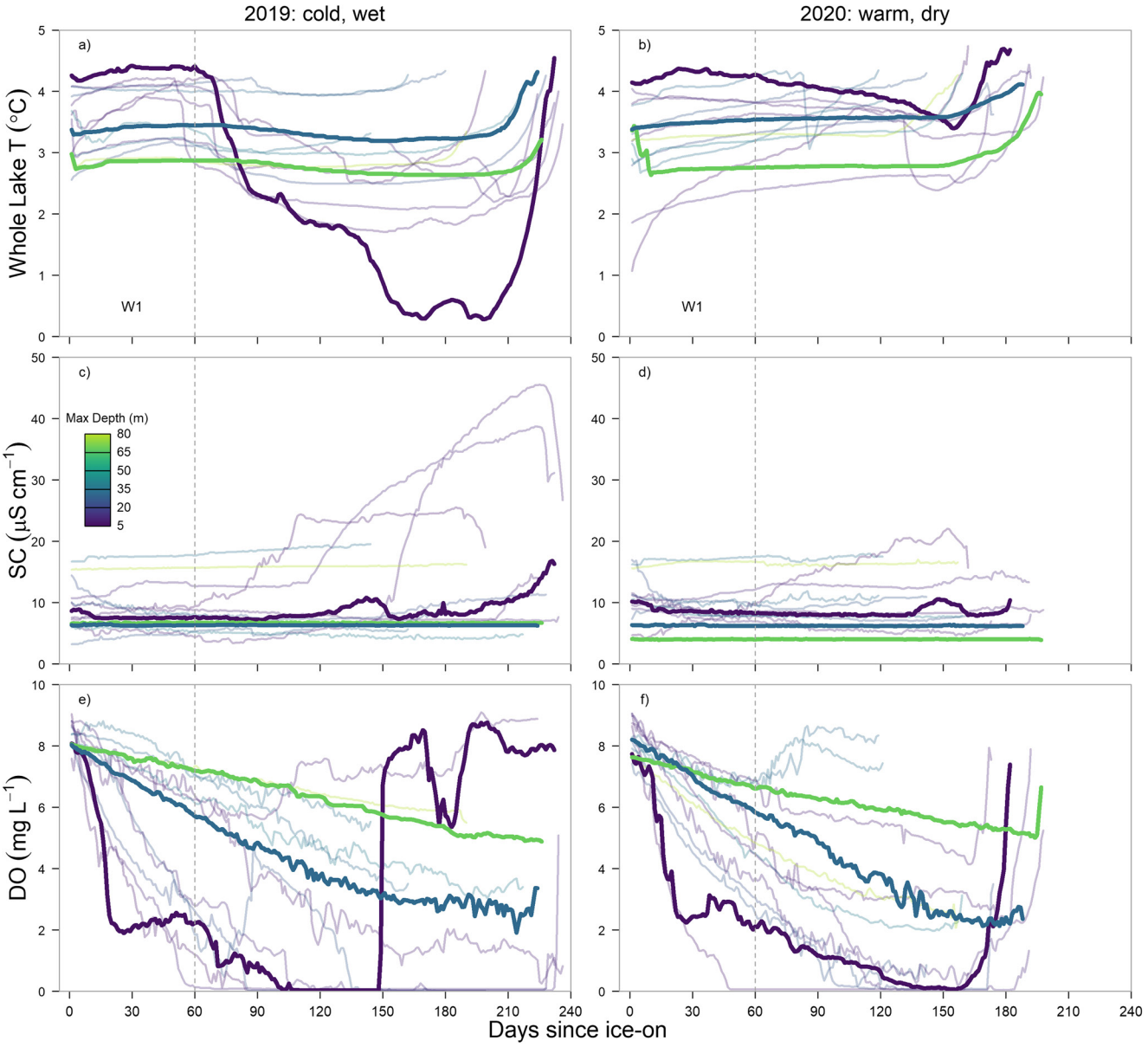


**Figure 5.** (a and b) Volume-weighted mean water temperature in WY 2019 and 2020, beginning on the first day of ice cover and ending at ice-off ($n = 14$ lakes; Swamp lake excluded). Vertical dashed lines mark the end of early winter (W1), defined as the 2 months following ice-on. Line colors correspond to maximum lake depth (m), from shallow (5 m, purple) to deep (80 m, yellow-green). (c and d) Near-bottom specific conductance (µS cm$^{-1}$). (e and f) Near-bottom DO concentration (mg L$^{-1}$). Bold lines show three high elevation lakes (>3,000 m.a.s.l.) of different maximum depths: shallow (Topaz, 5 m, purple line), intermediate (Ruby, 32.1 m, blue line), and deep (Ireland, 70.1 m, green line).

but hypoxic conditions lasted longer in WY 2019 than in 2020 (+23 additional days; $p < 0.05$, paired $t$-test). Shallow lakes tended to have a longer hypoxia duration than deep lakes (88 vs. 26 days; $p < 0.01$; Figure 7b).

### 3.6. Inter-Annual Variation in Emerald Lake

Variation in autumn and winter climate caused substantial variation in ice phenology and under-ice conditions at Emerald Lake over five winters (WY 2016–2020; Figure 8 and Table S1). Mean autumn air temperature ranged from 1.95 to 4.2°C. Warm autumn air temperatures in WY 2018 delayed the formation of seasonal ice cover by over a month (January 5) relative to the other 4 years (November 27 and 28; Figure 8). Before ice-formation in each year, maximum whole lake temperature ranged from 14.76 to 19.58°C, and

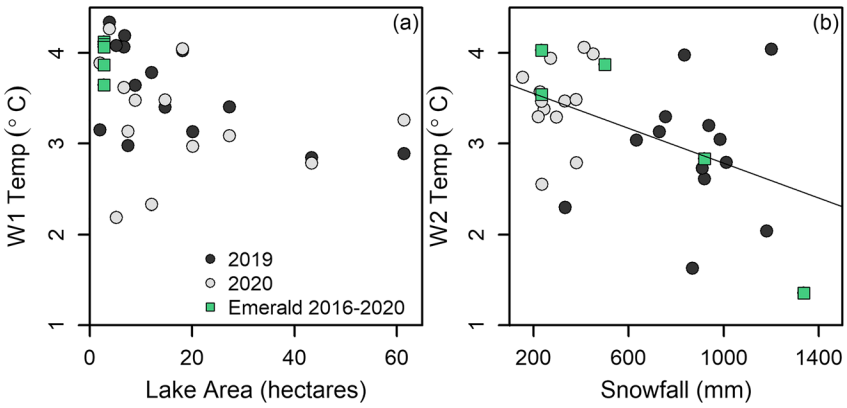


**Figure 6.** (a) Mean early winter (W1) lake temperature is more variable in small lakes. (b) Late winter lake temperature is related to the amount of winter snowfall (mm; black line shows regression relationship; $p < 0.01$; $R^2 = 0.21$), which prolongs the duration of ice cover. Green squares represent five winters (WY 2016–2020) in Emerald Lake. Two winters (WY 2019 and 2020) are shown for other lakes (black and gray dots).

the duration of fall mixing lasted from 30 to 73 days. Winter snowfall varied fivefold among years (233–1,336 mm), causing ice-off dates to vary by over 50 days (May 21–July 11), and ice duration to vary by almost 3 months (range 142–224 days, mean 189 days). The variation in ice phenology at Emerald Lake, however, was not substantially greater than exhibited by the other lakes in WY 2019 and WY 2020 (Figure 4). The timing of snowfall differed among years and influenced the seasonal progression of ice thickness and under-ice thermal and chemical conditions. Early or mid-winter snowstorms in 2017 and 2019 were followed by abrupt declines in water temperature, potentially because ice was submerged by the weight of overlying snow (dashed lines in Figures 8b and 8d). In low-snow years such as 2018 and 2020, late winter and spring precipitation may have triggered avalanches and snowmelt flows that appear as rapid changes in temperature, DO, and SC under ice (dashed lines in Figures 8c and 8e). In high snow years such as 2017 and 2019, snowmelt intrusions occurred during spring and were large enough relative to lake volume to completely mix the water column before ice-off (Figures 8b and 8d; Smits et al., 2020).

Inter-annual variation in under-ice water temperature at Emerald Lake (mean = 3.4°C, $SD$ = 0.8°C) was similar to the other small lakes (Topaz, Cottonwood 6, Clyde) and much larger than exhibited by deeper lakes. Lake temperature decreased during W1 in WY 2016–2018, but temperature increased during W1 in WY 2019–2020 (range $-0.026 \pm 0.0004$°C day$^{-1}$). Lake temperature decreased during W2 in all years (range $-0.01$ to $-0.003$°C day$^{-1}$). Early winter water temperature varied less than late winter water temperature ($SD$ = 0.2 vs. 1.0°C; Figures 6a and 6b).

DO depletion rates in Emerald Lake immediately following ice-on were similar among years (−0.03 to 0.05 mg L$^{-1}$ day$^{-1}$; Figure 7a and Table S2). Early winter DO concentration varied less than late winter concentrations among years. Mean W2 DO concentration (1.27–6.84 mg L$^{-1}$) varied more in Emerald Lake than in any of the other lakes (Table S1).

### 3.7. Regression Results

#### 3.7.1. Ice-On DOY

Deep lakes (maximum depth > 15 m) had later ice-on dates (+14 days), and ice-on was earlier at higher elevations, where autumn air temperatures were lower. The best model for ice-on DOY included mean autumn air temperature and lake depth class ($R^2 = 0.33$, $\Delta AIC_c > 8$; Table 2 summarizes regression results, complete AIC tables are found in Table S4). The best single predictors of ice-on DOY were mean autumn air temperature ($MeanAirT_{autumn}$; $R^2 = 0.24$, $\Delta AIC_c > 6$ compared to null model), elevation, lake depth class, and mean nighttime temperatures in autumn.

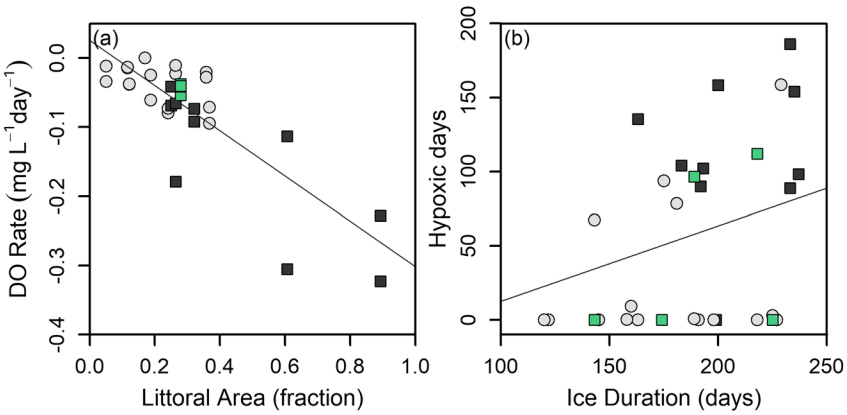


**Figure 7.** (a) Bottom water DO depletion rates after ice-on are greatest in shallow lakes (<15 m maximum depth; black squares) with a high fraction of littoral area relative to surface area, whereas deeper lakes (maximum depth > 15 m; gray dots) have low depletion rates. The black line shows the linear regression between littoral area and DO rate (Table 2). Green squares show Emerald lake rates for WY 2016–2020. (b) Duration of hypoxia (DO < 2 mg L$^{-1}$) increased with ice duration (Table 2). Note: Data from Swamp Lake are excluded.

**Table 2**
*Summary of Regression Model Results*

| Response | Climatic predictors | Intrinsic predictors | Dynamic lake predictors | Top model | $\Delta AIC_c$ | $R^2$ | $N$ |
|---|---|---|---|---|---|---|---|
| Ice-on DOY | $MeanAirT_{autumn}$ (+, 0.24)<br>$MinAirT_{autumn}$ (+, 0.14) | Elevation (−, 0.20)<br>DepthClass (+, 0.15) | None | $MeanAirT_{autumn}$ (+)<br>DepthClass (+) | 9.66 | 0.33 | 31; Swamp 2020, Skelton 2019 |
| Ice-off DOY | $MeanAirT_{winter}$ (−, 0.56)<br>$MeanAirT_{spring}$ (−, 0.26)<br>$Snow_{winter}$ (+, 0.24) | Elevation (+, 0.35)<br>Latitude (−, 0.10) | None | $MeanAirT_{winter}$ (−)<br>$Snow_{winter}$ (+) | 40.22 | 0.74 | 32; Swamp 2020 |
| Ice duration | $MeanAirT_{winter}$ (−, 0.57)<br>$MeanAirT_{spring}$ (−, 0.34)<br>$Snow_{winter}$ (+, 0.15) | Elevation (+, 0.44)<br>DepthClass (−, 0.12) | None | $MeanAirT_{winter}$ (−)<br>$Snow_{winter}$ (+)<br>DepthClass (−) | 36.50 | 0.71 | 33; none |
| W1 water temp | None | LakeSA (−, 0.16)<br>MaxDepth (−, 0.13)<br>MeanDepth (−, 0.12)<br>Volume (−, 0.10) | MaxTW (+, 0.14) | LakeSA (−) | 3.99 | 0.16 | 31; Swamp 2020, Skelton 2019 |
| W2 water temp | $Snow_{winter}$ (−, 0.21)<br>$MeanAirT_{winter}$ (+, 0.14) | None | IceOffDOY (−, 0.42)<br>IceDuration (−, 0.41) | IceOffDOY (−) | 15.60 | 0.42 | 31; Swamp 2019-2020 |
| DO depletion rate | None | LittoralSA (+, 0.66)<br>DepthClass (−, 0.21)<br>MeanDepth (−, 0.20)<br>MaxDepth (−, 0.18) | IceOn (−, 0.12) | LittoralSA (+) | 32.38 | 0.66 | 31; Swamp 2020, Skelton 2019 |
| Hypoxia duration | None | MaxDepth (−, 0.28)<br>MeanDepth (−, 0.26)<br>LakeSA (−, 0.23)<br>DepthClass (−, 0.23)<br>LittoralSA (+, 0.22)<br>Volume (−, 0.16) | DOSlope (+, 0.32)<br>IceDuration (+, 0.14) | DOSlope (+)<br>MaxDepth (−) | 13.13 | 0.40 | 31; Swamp 2020, Skelton 2019 |

*Note*. For each response variable, we report significant climatic, intrinsic (static lake or watershed), and dynamic lake predictor variables, the direction of their effect (positive or negative), and the variance explained ($R^2$). We also report predictors included in the best-fitting additive multiple regression model (Top Model), and metrics of fit for the best model. If multiple regression models did not improve AICc by more than 2 compared with the best single-predictor model, then the best single-predictor model is shown instead. ΔAICc was calculated relative to an intercept-only null model for each response variable. N is the number of lake-year combinations for each response variable with a complete set of predictor variables, and we report the lake-years missing from the regressions. MaxTW refers to maximum whole-lake temperature in the summer preceding the water year. SA refers to surface area. DepthClass is a categorical predictor (shallow: maximum lake depth < 15 m, deep: maximum lake depth > 15 m), and the direction of its effect refers to the "deep" category (e.g., deep lakes have later ice-on DOY, DepthClass effect is positive).

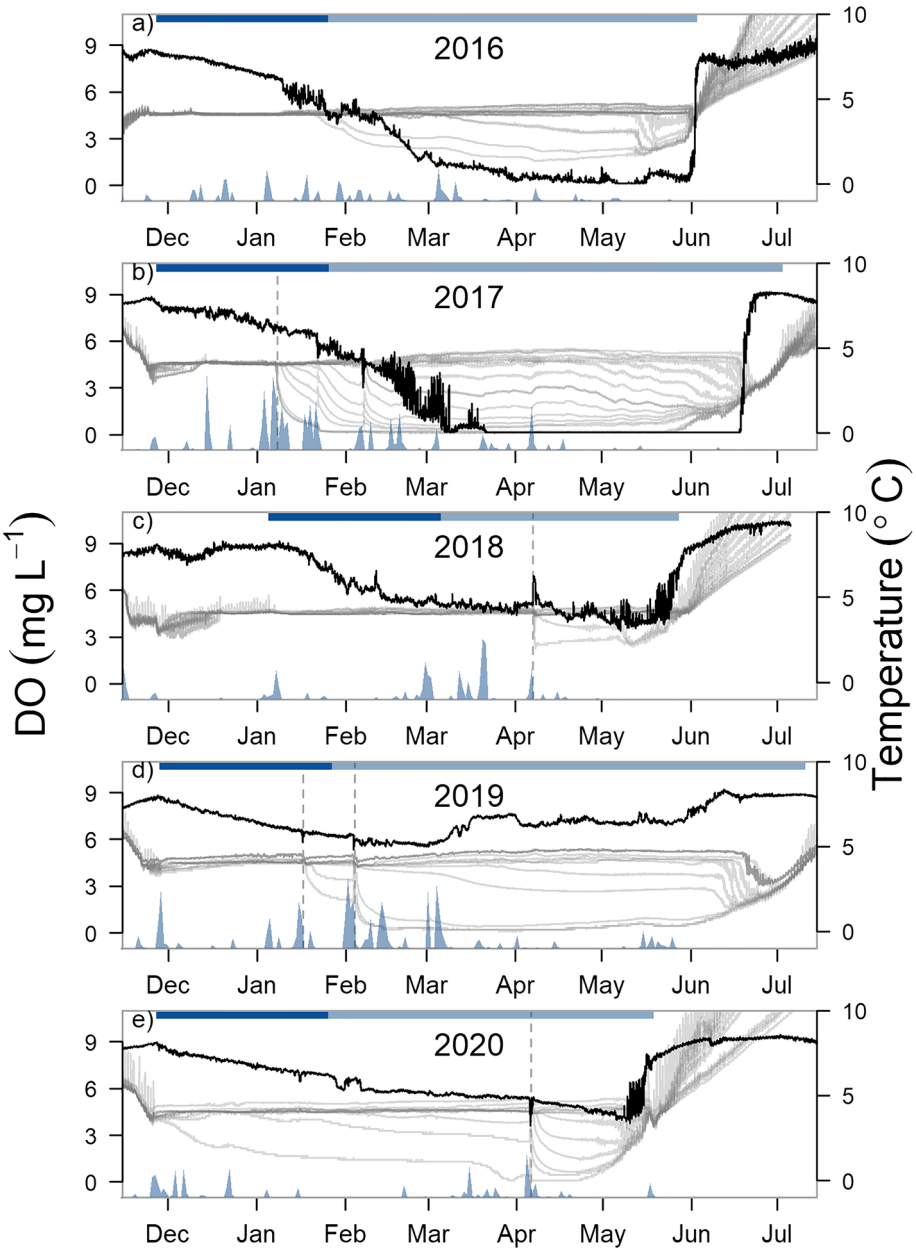


**Figure 8.** (a–e) Inter-annual variation (WY 2016–2020) in winter snowfall (blue time series; plotting range 0–300 mm), ice cover (blue bar), water temperature (gray lines), and bottom water DO (mg $L^{-1}$; black lines) in Emerald Lake. Dark blue portion of bar shows the time period corresponding to W1. In WY 2018 (c), an early ice cover developed in December but melted and re-formed in January. Dashed vertical lines in (b and d) show heavy snowfall resulting in lake temperature changes, likely due to ice submergence and mixing. Dashed lines in (c and e) show late winter precipitation that triggered rapid temperature and DO changes.

### 3.7.2. Ice-Off DOY

Spring climate variables were less important than winter climate variables for determining ice-off DOY. The best model for ice-off DOY included mean winter air temperature and winter snowfall ($R^2 = 0.74$, $\Delta AIC_c > 40$; Table 2). The best single predictor of ice-off DOY was mean air temperature during winter ($MeanAirT_{winter}$; $R^2 = 0.56$, $\Delta AIC_c > 20$), followed by elevation, mean air temperature during spring, cumulative snowfall during winter, and latitude.

#### 3.7.3. Ice Duration

The best multiple predictor model for ice duration included winter air temperature, winter snowfall, and lake depth class ($R^2$ = 0.71, $\Delta AIC_c > 30$; Table 2); deep lakes had shorter ice duration (−41 days), and excluding depth class from the model worsened $AIC_c$ by 5. The best single predictor of ice duration was mean winter air temperature ($R^2 = 0.57$, $\Delta AIC_c > 20$), followed by elevation, spring air temperature, winter snowfall, and lake depth class.

#### 3.7.4. W1 Water Temperature

None of the predictor variables explained substantial variation in W1 temperature. The single best predictor of under-ice water temperature in early winter was lake surface area ($R^2 = 0.16$, $\Delta AIC_c > 2$; Table 2), followed by maximum water temperature in summer, maximum depth, mean depth, and lake volume.

#### 3.7.5. W2 Water Temperature

W2 temperatures were related to winter climate variables that affected ice duration and ice-off date. Ice off DOY and ice duration were the two best single predictors of W2 temperature ($\Delta AIC_c > 10$, $R^2 = 0.42$; $\Delta AIC_c$, $R^2 = 0.41$; Table 2), followed by winter snowfall (Figure 6b) and mean winter air temperature.

#### 3.7.6. DO Depletion Rate

Rates of bottom water DO depletion immediately after ice-on were related to lake morphology and depth, rather than to climatic variables. The single best predictor of initial DO decline rate was a lake's percent littoral area (LittoralSA; $R^2 = 0.66$, $\Delta AIC_c > 30$; Table 2 and Figure 7a), followed by lake depth class (deep lakes had lower DO depletion rates; Figure 7a), mean depth, maximum depth, and ice-on DOY.

#### 3.7.7. Duration of Hypoxia

The overall best model for bottom-water hypoxia duration included the initial rate of oxygen depletion under ice (DOSlope) and maximum depth ($R^2 = 0.40$, $\Delta AIC_c > 10$; Table 2), though a model with DOSlope and ice duration fit equally well ($R^2 = 0.40$, $\Delta AIC_c > 10$; Figure 7b). The best single predictors of hypoxia duration were DOSlope ($R^2 = 0.32$, $\Delta AIC_c > 10$), maximum lake depth, and mean lake depth, followed by lake surface area, depth class (deep lakes had shorter hypoxia duration, −62 days), percent littoral area, lake volume, and ice duration.

## 4. Discussion

We used multiple years of high-frequency measurements from 15 morphologically diverse lakes in California to characterize drivers of ice cover and under-ice thermal and chemical conditions in a mid-latitude, snow-dominated mountain landscape. We aimed to evaluate how well conceptual models of under-ice dynamics developed in cold, high latitude regions (e.g., Winter I and Winter II; Kirillin et al., 2012) described the behavior of lakes subject to warm air temperatures and substantial inter-annual variation in snowfall. While lake surface area varied by an order of magnitude among our study sites (2–60 ha) and was representative of typical lake sizes in the Sierra Nevada (Melack et al., 2021) and the most abundant range of lake sizes globally (Downing et al., 2006), all were relatively small, and our study was focused on dynamics within these representative lake types. We found that winter air temperature and snow accumulation were associated with ice-off timing and ice cover duration, but that lake morphology and depth influenced ice-on timing and subsequent DO depletion rates. Processes affected by ice duration, such as late winter water temperature and the duration of bottom-water hypoxia, were indirectly affected by winter climate variables. Shallow lakes responded more directly to snowfall than deeper lakes, exhibiting large changes in temperature, DO, and SC under ice (Figure 5), likely because a larger fraction of their total volume was influenced by ice and snow submergence or meltwater inflows. Dynamics resembling Winter I (e.g., "dark mode") were the predominant condition in most lakes due to the contribution of snowfall to lake ice cover across elevations. "Winter II" conditions (radiation-driven convection and mixing) likely occurred for short periods in most lakes, such as after ice-on but before the first snowfall, or during spring snowmelt. Winter II conditions also likely occurred for multiple weeks in mid-winter during the dry WY 2020, both in low elevation lakes (Castle, Cliff, Miller, Boundary), and in several deeper high elevation lakes (Big Bird, Dorothy), as evidenced by increases in sub-surface light intensity (Figure S3). Given predicted increases in air

temperature and declines in winter snow in the Sierra Nevada (Cayan et al., 2008; Fyfe et al., 2017), shallow lakes (<15 m depth) and lakes at low elevations may see more dramatic changes in thermal and chemical conditions. However, deeper lakes, or those situated in catchments with greater radiation or wind exposure, may be at greater risk of reduced ice thickness and shorter ice-cover duration, and may exhibit more Winter II dynamics in the future.

### 4.1. Drivers of Ice-Phenology

Inter-annual and spatial variation in ice phenology of mountain lakes in California was driven by ice-off timing rather than ice formation timing (Figure 4). Consequently, ice phenology and ice duration responded most directly to winter snowfall and air temperature (Table 2), as has been observed in boreal lakes (Schindler et al., 1990), rather than to autumn or spring climate variables (Preston et al., 2016). Lake and watershed characteristics had minimal effects on ice phenology, though deeper lakes had later ice-on dates.

Although ice-formation is thought to be more responsive to synoptic weather events than ice breakup (Kirillin et al., 2012), ice-on timing was relatively invariant among years in the study lakes—on average ice-on DOY varied by only 4 days between years. Autumn air temperature, which relates to latent, sensible, and radiative heat loss fluxes from lakes (MacIntyre & Melack, 2009; Woolway et al., 2018), explained more variation in ice-formation timing than any other single variable ($R^2$ = 0.24; Table 2). However, the best regression model explained less than half the variation ($R^2$ = 0.33), indicating that important processes were not captured by our predictor set. Synoptic weather patterns can play a large role in ice-on timing (Kirillin et al., 2012), but we lacked local wind or radiation data needed to model autumn heat fluxes from lakes. However, the invariance of ice-on DOY among years indicates that individual weather events play a smaller role in temperate high elevation lakes than is true for regions with more variable or extreme autumn weather. Rather, intrinsic characteristics such as a lake's heat capacity (i.e., volume) or susceptibility to wind-driven or convective heat losses (i.e., surface area, watershed slope, and aspect) may explain additional variation among lakes at a given elevation. Lake surface area (fetch, exposure of lake surface to radiation), lake mean depth (total heat capacity and propensity for efficient mixing and heat loss), and topography (solar shading, wind-blocking) should all influence autumn heat losses from lakes, but these characteristics are often correlated and their effects difficult to distinguish using regression models. The late ice-on DOY at Emerald Lake in WY 2018 indicates that anomalously warm autumn air temperatures, which are occurring more frequently in California (Goss et al., 2020), may substantially delay ice formation in lakes where it has previously been temporally stable.

We expected ice-off timing to be determined by winter climate variables associated with snowpack magnitude (precipitation and air temperature), as well as by spring climatic conditions associated with snowmelt (air temperature, precipitation, and radiation; Preston et al., 2016). We found that winter climate variables were more predictive of ice-off date than spring climate variables, in contrast to findings for Rocky Mountain lakes, where spring climate variables (April–June) determined ice-off dates (Preston et al., 2016). Our results agree with those of Caldwell et al. (2020), who found that winter air temperature and snowpack were more predictive of ice-off timing than spring variables in western US mountain lakes >1 km$^2$, indicating that the magnitude of energy needed to melt the accumulated snow and ice cover is more important than spring weather conditions (e.g., incoming heat fluxes) for ice-off timing in systems where winter snow can be many meters deep.

We expected lake or watershed attributes that influence snow thickness or retention on lake ice to modify ice-off timing. For example, wind scour and exposure to solar radiation reduce snow thickness and may be more prevalent on lakes with larger surface area and fetch. Therefore, both the albedo and thickness of ice cover on larger lakes may be lower, promoting earlier ice breakup than for smaller lakes at the same elevation. Topographic shading in steep, north-facing basins blocks incoming radiation needed to melt snow, delaying snowmelt and potentially ice-off, especially in smaller lakes where shading affects more of the total lake surface. However, variables related to lake size, morphology, or topographic shading did not improve model fits to the ice-off data, in contrast to a study of high elevation lakes in the Tatra Mountains (Novikmec et al., 2013), where both lake depth and radiative inputs were related to ice-off dates. Given the strong theoretical relationship between solar radiation and rates of snow and ice melt (Leppäranta, 2015), we were surprised by this finding, but lack of significance in regression models may reflect the complexity of processes

affecting snow retention and melt in mountainous terrain (Tennant et al., 2017). Further, we used gridded climate products (4 km resolution) to estimate snowfall at each lake because site-specific measurements were unavailable, whereas true snowfall and snow retention may have differed substantially. Finally, our study lakes may have been too small to show significant variation in ice breakup dynamics related to wind forcing or the degree of surface shading.

### 4.2. Factors Regulating Winter Thermal Dynamics

Controls on under-ice thermal conditions diverged between early and late winter: lake temperature in early winter was not related to climate variables, whereas late winter lake temperature was related to winter climate variables and ice cover duration (Figure 6 and Table 2). For W1 lake temperature (volume-weighted mean), we expected climatic or morphometric variables related to autumn heat losses, mixing, and ice-on timing would be influential by setting the starting lake temperature at ice-on. We also expected variables related to the magnitude of sediment heating in summer, and thus the magnitude of sediment heat flux in early winter, to determine lake warming under ice. Small, shallow lakes with extensive littoral zones should have the largest sediment heat fluxes and warming rates because their sediments are directly exposed to solar radiation during summer, and a greater proportion of lake volume is in contact with sediments. Large, deep lakes should warm less after ice-on due to their greater volume and relatively smaller littoral zones. Contrary to our expectations, we found no relationships between W1 water temperature and autumn climate variables or ice-on DOY, and only very weak effects of lake size or morphology (surface area, depth, and volume; Figure 6 and Table 2). The fact that no predictors explained much variation in W1 water temperature may be related to the low among-lake variation in W1 temperature, with lake temperatures rarely colder than 3°C, in contrast to lakes at higher latitudes that can approach 0°C at ice-on (Terzhevik et al., 2009). Alternatively, the range of lake sizes in our study was small (2–60 ha), potentially limiting our ability to detect relationships between lake size and W1 temperature.

Ice and snow thickness and duration are intrinsically related, but they can affect late winter lake temperature through several different mechanisms. Ice duration, ice-off DOY, and winter climate variables were the best predictors of late winter lake temperatures. Snow prolongs ice cover by contributing thermal mass needing to be melted, and by increasing the albedo of the ice (Caldwell et al., 2020; Sánchez-López et al., 2015). Thick snow shields lakes from incoming solar radiation during late winter and spring, delaying ice breakup and the onset of lake warming (Smits et al., 2020). This is likely a significant factor controlling late winter water temperature in temperate mountain lakes, which can experience winter air temperatures above 0°C and substantial incoming shortwave radiation (Sadro et al., 2018a). Heavy snowfall can submerge lake ice below the water level where it melts, decreasing water temperatures in shallow lakes such as Emerald (Figure 8). In Emerald Lake, high snowfall reduced late winter temperatures (Figure 6b; green squares), but there was no significant effect of lake depth on late winter temperature in the larger data set. Ultimately, winter snowfall probably affects lake temperature both by prolonging ice cover and shielding lakes from incoming radiation, and also by contributing directly to ice submergence or snowmelt intrusions under ice in shallow lakes.

### 4.3. Drivers of Under-Ice Oxygen Dynamics

Lake morphology, specifically the extent of shallow littoral areas relative to the total surface area, was the main driver of early winter oxygen dynamics in California mountain lakes (Figure 7a), similar to findings from high latitude lakes in Alaska and Canada (Leppi et al., 2016; Mathias & Barica, 1980; Meding & Jackson, 2003). Initial rates of bottom-water DO depletion after ice-on varied considerably among lakes (−0.0001 to 0.322 mg $L^{-1}$ $day^{-1}$; Figure 7a), but within lakes, rates were similar across years. Intrinsic features related to the size of the DO pool (e.g., lake volume) and accumulation of sediments in littoral zones (mean depth and percent littoral area), rather than temporal variation in climatic conditions, dictated oxygen depletion rates after ice-on. In small oligotrophic mountain lakes, under-ice oxygen depletion can approach rates found in eutrophic systems but generally does not vary among years (Granados et al., 2020; but see Obertegger et al., 2017), perhaps because microbial communities are cold-adapted and do not respond to small differences in water temperature (Bertilsson et al., 2013). Despite demonstrated temperature dependence of lake sediment respiration (Gudasz et al., 2010; Sobek et al., 2017), especially at low temperatures

(Den Heyer & Kalff, 1998; Graneli, 1978; Hargrave, 1969), bottom water temperature had no relation to DO depletion rates in our study, supporting findings that watershed attributes such as vegetation cover or nutrient loading are more important factors at regional scales (Clow et al., 2015). Shallow lakes at high (Topaz) and low elevations (Miller) had high DO depletion rates (>0.1 mg $L^{-1}$ $day^{-1}$), indicating that despite likely differences in organic matter (OM) sources and composition, sediment pools of OM were sufficiently high to fuel comparable rates of respiration. We did not measure the organic matter content of lake sediments, which can influence microbial respiration rates and thus DO consumption (Terzhevik et al., 2009). Macrophytes and terrestrial particulate OM probably contributed a majority of the OM to littoral sediments in low elevation lakes, driving rapid DO depletion under ice (Meding & Jackson, 2003). Littoral zones in high elevation lakes above tree-line can also contain organic-rich sediments due to benthic algae and phytoplankton production (Bunting et al., 2010; Gudasz et al., 2017; Thevenon et al., 2012), fueling microbial respiration and DO depletion at rates similar to lower elevation lakes with greater terrestrial OM loading.

Initial rates of oxygen depletion under ice, and thus the likelihood of a lake bottom developing hypoxia, were primarily determined by lake depth and morphology (Figure 7a). However, late winter DO concentrations were also influenced by winter climate variation, although the mechanisms linking winter air temperature and precipitation to DO dynamics differed between deep and shallow lakes. DO declined steadily throughout winter in the deepest lakes (e.g., Dorothy, Ireland, Figures 2, 3, 5e, and 5f); late winter DO concentrations were therefore directly determined by the duration of ice cover, and indirectly by winter air temperature and snowfall. In shallow lakes, DO often declined rapidly during early winter, quickly leading to hypoxic bottom waters; hypoxia duration was also directly related to ice cover duration in these lakes (Figure 7b). However, in some shallow lakes such as Emerald and Topaz, DO increased before ice-off following precipitation events (Figure 8c, dashed line) or during snowmelt (Figures 2, 8b, and 8d Topaz), which can precede ice-off by more than a month in wet years (Smits et al., 2020). Mixing associated with snowmelt inflows or ice and snow submergence are more likely explanations for these winter DO increases in shallow lakes than under-ice primary production, as they occurred concurrently with changes in lake temperature but without increases in sub-surface light intensity (Figures 2, 8, and S2).

### 4.4. Sensitivity of Mountain Lakes to Changes in Winter Climate

Temperate mountain lakes will experience earlier ice-off and shortened ice duration in the future (Caldwell et al., 2020; Sadro et al., 2018a). As the ice-covered period contracts, climatic factors during autumn and spring will increasingly determine ice phenology and under-ice processes. Warmer air temperatures in autumn will delay ice formation in most lakes, extending the ice-free period into winter months during which storms typically occur in California. As a result, ice formation may also become more responsive to synoptic weather patterns, and thus more variable among years. Shifts in the relative importance of climate variables controlling lake warming during summer are already apparent in low snow years (Smits et al., 2020), but we know little about how the loss of snow will affect climatic controls on ice cover and under-ice processes in mountain lakes.

Winter-time DO dynamics in mountain lakes are likely to change as ice duration shortens, the light transmissivity of ice increases with reduced snow cover, water temperature increases, and OM sources and loading change. Low snow-cover and mid-winter ice-thinning may allow for sustained primary production under the ice throughout winter (Maier et al., 2019; Obertegger et al., 2017; Salmi & Salonen, 2016), elevating DO in the upper water column. Increased radiation-driven convective mixing will oxygenate deeper parts of lakes, reducing bottom-water hypoxia. Though we did not find a significant relationship between water temperature and DO depletion rates, warmer water temperature may increase sediment respiration rates (Sobek et al., 2017), partly counter-acting the effects of mixing and phytoplankton productivity on DO. Rates of DO depletion during early winter may be higher if terrestrial OM loading to littoral zones or in-situ primary production during summer increase, or if winter rainfall results in OM loading. However, it seems more likely that winter DO concentrations will increase in most mountain lakes with reduced or intermittent ice and snow cover. Higher DO may benefit overwintering aquatic organisms such as fish and amphibians, but will also shift redox conditions under ice, altering nitrogen and carbon cycling (Denfeld et al., 2018; Powers et al., 2017). Shortened duration of hypoxia will reduce anaerobic respiration pathways such as methanogenesis and lower methane production, but greater $O_2$ availability may also facilitate overall higher

$CO_2$ emissions at ice-off. Currently, it remains unclear how reduced ice cover and elevated DO will change the annual carbon balance of temperate mountain lakes.

Temperature and DO respond differently to snowfall in deep and shallow mountain lakes, indicating that lake depth will determine the magnitude and direction of changes in winter processes with reduced snow and ice cover. Larger, deeper mountain lakes may experience greater reductions in ice duration and thickness, shifting from a predominantly dark, snow-covered mode to more frequent episodes of thin, clear ice that allow for convective mixing, photosynthesis, and higher DO concentrations. In contrast, many small, shallow lakes, especially at high elevation, are likely to retain snow cover because of topographic shading and protection from wind, and thus will probably continue to show "Winter I" type dynamics into the future, albeit for shorter duration. The bottom-waters of shallow lakes display more inter-annual variation in thermal and DO dynamics than those in deeper lakes, but they may become less variable in the future as the likelihood of heavy snowfall decreases. Without the episodic mixing caused by submergence of ice cover during snowstorms, late winter water temperature in small, shallow lakes will warm and bottom water DO will remain low. Alternatively, more frequent rain-on-snow events may increase mid-winter melt inflows, resulting in mixing and DO replenishment, though these dynamics will depend on lake morphology, antecedent thermal stratification, and organic matter loading associated with runoff. As more than 95% of lakes in the Sierra Nevada are smaller than 15 ha (Melack et al., 2021), understanding the responses of small mountain lakes to warming winters is especially crucial for predicting lake ecosystem functioning at a regional scale. Future work should focus on understanding mechanistic relationships between winter climate variation and thermal and chemical dynamics in temperate mountain lakes, and how lake size and morphology mediates those relationships.

## Data Availability Statement

Climate metrics, ice phenology data, and lake thermal and chemical data for all study lakes (Table S1) are available at the Environmental Data Initiative repository (Smits, 2021).

**Acknowledgments**
A. P. Smits was supported by an NSF EAR postdoctoral fellowship award (EAR-1725266). The authors thank E. Suenaga, M. J. Farruggia, G. DeLaRosa, B. Currinder, R. Knapp, and T. Karin for assistance with fieldwork and data collection.

## References

Abatzoglou, J. T. (2013). Development of gridded surface meteorological data for ecological applications and modelling. *International Journal of Climatology*, *33*(1), 121–131. https://doi.org/10.1002/joc.3413

Arp, C. D., Jones, B. M., & Grosse, G. (2013). Recent lake ice-out phenology within and among lake districts of Alaska, U.S.A. *Limnology and Oceanography*, *58*(6), 2013–2028. https://doi.org/10.4319/lo.2013.58.6.2013

Bertilsson, S., Burgin, A., Cayelan, C. C., Fey, S. B., Grossar, H.-P., Grubisic, L. M., et al. (2013). The under-ice microbiome of seasonally frozen lakes. *Limnology and Oceanography*, *58*(6). https://doi.org/10.4319/lo.2013.58.6.1998

Block, B. D., Denfeld, B. A., Stockwell, J. D., Flaim, G., Grossart, H. P. F., Knoll, L. B., et al. (2019). The unique methodological challenges of winter limnology. *Limnology and Oceanography: Methods*, *17*(1), 42–57. https://doi.org/10.1002/lom3.10295

Bunting, L., Leavitt, P. R., Weidman, R. P., & Vinebrookeb, R. D. (2010). Regulation of the nitrogen biogeochemistry of mountain lakes by subsidies of terrestrial dissolved organic matter and the implications for climate studies. *Limnology and Oceanography*, *55*(1), 333–345. https://doi.org/10.4319/lo.2010.55.1.0333

Burnham, K. P., & Anderson, D. R. (2002). Avoiding pitfalls when using information-theoretic methods. *Journal of Wildlife Management*, *66*(3), 912–918.

Caldwell, T. J., Chandra, S., Albright, T. P., Harpold, A. A., Dilts, T. E., Greenberg, J. A., et al. (2020). Drivers and projections of ice phenology in mountain lakes in the western United States. *Limnology and Oceanography*, *66*(3), 955–1008. https://doi.org/10.1002/lno.11656

Cayan, D. R., Maurer, E. P., Dettinger, M. D., Tyree, M., & Hayhoe, K. (2008). Climate change scenarios for the California region. *Climatic Change*, *87*, 21–42. https://doi.org/10.1007/s10584-007-9377-6

Clow, D. W., Stackpoole, S. M., Verdin, K. L., Butman, D. E., Zhu, Z., Krabbenhoft, D. P., & Striegl, R. G. (2015). Organic carbon burial in lakes and reservoirs of the conterminous United States. *Environmental Science and Technology*, *49*(13), 7614–7622. https://doi.org/10.1021/acs.est.5b00373

Den Heyer, C., & Kalff, J. (1998). Organic matter mineralization rates in sediments: A within- and among-lake study. *Limnology and Oceanography*, *43*(4), 695–705. https://doi.org/10.4319/lo.1998.43.4.0695

Denfeld, B. A., Baulch, H. M., del Giorgio, P. A., Hampton, S. E., & Karlsson, J. (2018). A synthesis of carbon dioxide and methane dynamics during the ice-covered period of northern lakes. *Limnology and Oceanography Letters*, *3*, 117–131. https://doi.org/10.1002/lol2.10079

Dettinger, M., Udall, B., & Georgakakos, A. (2015). Western water and climate change. *Ecological Applications*, *25*(8), 2069–2093. https://doi.org/10.1890/15-0938.1

Dingman, S. L. (2002). *Physical hydrology*. Prentice Hall.

Downing, J. A., Prairie, Y. T., Cole, J., Duarte, C. M., Tranvik, L. J., Striegl, R. G., et al. (2006). Abundance and size distribution of lakes, ponds and impoundments. *Limnology and Oceanography*, *51*(5). https://doi.org/10.1016/B978-0-12-409548-9.03867-7

Dozier, J., & Frew, J. (1990). Rapid calculation of terrain parameters for radiation modeling from digital elevation data. *IEEE Transactions on Geoscience and Remote Sensing*, *28*(5), 963–969. https://doi.org/10.1109/36.58986

Flaim, G., Andreis, D., Piccolroaz, S., & Obertegger, U. (2020). Ice cover and extreme events determine dissolved oxygen in a Placid Mountain Lake. *Water Resources Research*, *56*(9), 1–18. https://doi.org/10.1029/2020wr027321

Fyfe, J. C., Derksen, C., Mudryk, L., Flato, G. M., Santer, B. D., Swart, N. C., et al. (2017). Large near-term projected snowpack loss over the western United States. *Nature Communications*, *8*, 1–7. https://doi.org/10.1038/ncomms14996

Goss, M., Swain, D. L., Abatzoglou, J. T., Sarhadi, A., Kolden, C. A., Williams, A. P., & Diffenbaugh, N. S. (2020). Climate change is increasing the likelihood of extreme autumn wildfire conditions across California. *Environmental Research Letters*, *15*(9), 094016. https://doi.org/10.1088/1748-9326/ab83a7

Granados, I., Toro, M., Giralt, S., Camacho, A., & Montes, C. (2020). Water column changes under ice during different winters in a mid-latitude Mediterranean high mountain lake. *Aquatic Sciences*, *82*(30). https://doi.org/10.1007/s00027-020-0699-z

Graneli, W., & Graneli, W. (1978). Sediment oxygen uptake in South Swedish Lakes. *Oikos*, *30*(1), 7–16. https://doi.org/10.2307/3543519

Gudasz, C., Bastviken, D., Steger, K., Premke, K., Sobek, S., & Tranvik, L. J. (2010). Temperature-controlled organic carbon mineralization in lake sediments. *Nature*, *466*(7305), 478–481. https://doi.org/10.1038/nature09186

Gudasz, C., Ruppenthal, M., Kalbitz, K., Cerli, C., Fiedler, S., Oelmann, Y., et al. (2017). Contributions of terrestrial organic carbon to northern lake sediments. *Limnology and Oceanography Letters*, *2*(6), 218–227. https://doi.org/10.1002/lol2.10051

Hampton, S. E., Galloway, A. W. E., Powers, S. M., Ozersky, T., Woo, K. H., Batt, R. D., et al. (2017). Ecology under lake ice. *Ecology Letters*. *20*(1). https://doi.org/10.1111/ele.12699

Hargrave, B. T. (1969). Epibenthic algal production and community respiration in the sediments of Marion Lake. *Journal of the Fisheries Research Board of Canada*, *26*(8), 2003–2026. https://doi.org/10.1139/f69-189

Harpold, A. A., & Brooks, P. D. (2018). Humidity determines snowpack ablation under a warming climate. *Proceedings of the National Academy of Sciences of the United States of America*, *115*(6), 1215–1220. https://doi.org/10.1073/pnas.1716789115

Harpold, A. A., Dettinger, M., & Rajagopal, S. (2017). Defining snow drought and why it matters. *Eos, Transactions American Geophysical Union*, *98*(5), 15–17. https://doi.org/10.1029/2017eo068775

Hyndman, R., Athanasopoulos, G., Bergmeir, C., Caceres, G., Chhay, L., O'Hara-Wild, M., et al. (2020). *Forecasting functions for time series and linear models*.

Killick, R., Haynes, K., & Eckley, I. (2016). *Methods for changepoint detection*.

Kirillin, G., Leppäranta, M., Terzhevik, A., Granin, N., Bernhardt, J., Engelhardt, C., et al. (2012). Physics of seasonally ice-covered lakes: A review. *Aquatic Sciences*, *74*(4), 659–682. https://doi.org/10.1007/s00027-012-0279-y

Leppäranta, M. (2015). *Freezing of lakes and the evolution of their ice cover*. Springer Berlin Heidelberg. https://doi.org/10.1007/978-3-642-29081-7

Leppi, J. C., Arp, C. D., & Whitman, M. S. (2016). Predicting late winter dissolved oxygen levels in Arctic Lakes using morphology and landscape metrics. *Environmental Management*, *57*(2), 463–473. https://doi.org/10.1007/s00267-015-0622-x

MacIntyre, S., & Melack, J. M. (2009). Mixing dynamics in lakes across climatic zones. In *Encyclopedia of inland waters* (pp. 603–612). https://doi.org/10.1016/b978-012370626-3.00040-5

Magnuson, J. J., Robertson, D. M., Benson, B. J., Wynne, R. H., Livingstone, D. M., Arai, T., et al. (2000). Historical trends in lake and river ice cover in the Northern Hemisphere. *Science*, *289*(5485), 1743–1746. https://doi.org/10.1126/science.289.5485.1743

Maier, D. B., Diehl, S., & Bigler, C. (2019). Interannual variation in seasonal diatom sedimentation reveals the importance of late winter processes and their timing for sediment signal formation. *Limnology and Oceanography*, *64*(3), 1186–1199. https://doi.org/10.1002/lno.11106

Mathias, J. A., & Barica, J. (1980). Factors controlling oxygen depletion in ice-covered lakes. *Canadian Journal of Fisheries and Aquatic Sciences*, *37*(2), 185–194. https://doi.org/10.1139/f80-024

Mazerolle, M. J. (2020). *AICcmodavg: Model selection and multi-model inference based on AICc*. Retrieved from https://cran.r-project.org/package=AICcmodavg

Meding, M. E., & Jackson, L. J. (2003). Biotic, chemical, and morphometric factors contributing to winter anoxia in prairie lakes. *Limnology and Oceanography*, *48*(4), 1633–1642. https://doi.org/10.4319/lo.2003.48.4.1633

Melack, J. M., Sadro, S., Sickman, J. O., & Dozier, J. (2021). *Lakes and watersheds in the Sierra Nevada of California: Responses to environmental change*. University of California Press.

Novikmec, M., Svitok, M., Kočický, D., Šporka, F., & Bitušík, P. (2013). Surface water temperature and ice cover of Tatra Mountains Lakes depend on altitude, topographic shading, and bathymetry. *Arctic Antarctic, and Alpine Research*, *45*(1), 77–87. https://doi.org/10.1657/1938-4246-45.1.77

Obertegger, U., Obrador, B., & Flaim, G. (2017). Dissolved oxygen dynamics under ice: Three winters of high-frequency data from Lake Tovel, Italy. *Water Resources Research*, *53*, 7234–7246. https://doi.org/10.1002/2017WR020599

Oleksy, I. A., Beck, W. S., Lammers, R. W., Steger, C. E., Wilson, C., Christianson, K., et al. (2020). The role of warm, dry summers and variation in snowpack on phytoplankton dynamics in mountain lakes. *Ecology*, *101*(10), 1–12. https://doi.org/10.1002/ecy.3132

Pepin, N., Bradley, R. S., Diaz, H. F., Baraer, M., Caceres, E. B., Forsythe, N., et al. (2015). Elevation-dependent warming in mountain regions of the world. *Nature Climate Change*, *5*. https://doi.org/10.1038/nclimate2563

Pernica, P., North, R. L., & Baulch, H. M. (2017). In the cold light of day: The potential importance of under-ice convective mixed layers to primary producers. *Inland Waters*, *7*(2), 138–150. https://doi.org/10.1080/20442041.2017.1296627

Pierson, D. C., Weyhenmeyer, G. A., Arvola, L., Benson, B., Blenckner, T., Kratz, T., et al. (2011). An automated method to monitor lake ice phenology. *Limnology and Oceanography: Methods*, *9*, 74–83. https://doi.org/10.4319/lom.2010.9.0074

Powers, S. M., Labou, S. G., Baulch, H. M., Hunt, R. J., Lottig, N. R., Hampton, S. E., & Stanley, E. H. (2017). Ice duration drives winter nitrate accumulation in north temperate lakes. *Limnology and Oceanography Letters*, *2*(5), 177–186. https://doi.org/10.1002/lol2.10048

Preston, D. L., Caine, N., McKnight, D. M., Williams, M. W., Hell, K., Miller, M. P., et al. (2016). Climate regulates alpine lake ice cover phenology and aquatic ecosystem structure. *Geophysical Research Letters*, *43*(10), 5353–5360. https://doi.org/10.1002/2016GL069036

R Core Team. (2015). *R: A language and environment for statistical computing*. R Foundation for Statistical Computing Vienna.

Read, J. S., Hamilton, D. P., Jones, I. D., Muraoka, K., Winslow, L. A., Kroiss, R., et al. (2011). Derivation of lake mixing and stratification indices from high-resolution lake buoy data. *Environmental Modelling and Software*, *26*(11), 1325–1336. https://doi.org/10.1016/j.envsoft.2011.05.006

Rue, G. P., Darling, J. P., Graham, E., Tfaily, M. M., & McKnight, D. M. (2020). Dynamic changes in dissolved organic matter composition in a mountain lake under ice cover and relationships to changes in nutrient cycling and phytoplankton community composition. *Aquatic Sciences*, *82*(1), 1–16. https://doi.org/10.1007/s00027-019-0687-3

Sadro, S., Melack, J. M., Sickman, J. O., & Skeen, K. (2018a). Climate warming response of mountain lakes affected by variations in snow. *Limnology and Oceanography Letters*, *4*, 9–17. https://doi.org/10.1002/lol2.10099

Sadro, S., Melack, J. M., Sickman, J. O., & Skeen, K. (2018b). Effects of climate variability on snowmelt and implications for organic matter in a high-elevation lake. *Water Resources Research*, *54*(7), 4563–4578. https://doi.org/10.1029/2017WR022163

Salmi, P., & Salonen, K. (2016). Regular build-up of the spring phytoplankton maximum before ice-break in a boreal lake. *Limnology and Oceanography*, *61*(1), 240–253. https://doi.org/10.1002/lno.10214

Sánchez-López, G., Hernández, A., Pla-Rabes, S., Toro, M., Granados, I., Sigró, J., et al. (2015). The effects of the NAO on the ice phenology of Spanish alpine lakes. *Climatic Change*, *130*(2), 101–113. https://doi.org/10.1007/s10584-015-1353-y

Schindler, D. W., Beaty, K. G., Fee, E. J., Cruikshank, D. R., DeBruyn, E. R., Findlay, D. L., et al. (1990). Effects of climatic warming on lakes of the Central Boreal Forest. *Science*, *250*(4983), 967–970. https://doi.org/10.1126/science.250.4983.967

Sharma, S., Blagrave, K., Magnuson, J. J., O'Reilly, C. M., Oliver, S., Batt, R. D., et al. (2019). Widespread loss of lake ice around the Northern Hemisphere in a warming world. *Nature Climate Change*. *9*, 227–231. https://doi.org/10.1038/s41558-018-0393-5

Smits, A. P. (2021). *Ice phenology and under-ice temperature and oxygen data for lakes of the CA ver 1*. Environmental Data Initiative. https://doi.org/10.6073/pasta/7ce27646dc4e31c1e5cb9f7a93418430

Smits, A. P., MacIntyre, S., & Sadro, S. (2020). Snowpack determines relative importance of climate factors driving summer lake warming. *Limnology and Oceanography Letters*, *5*, 271–279. https://doi.org/10.1002/lol2.10147

Sobek, S., Gudasz, C., Koehler, B., Tranvik, L. J., Bastviken, D., & Morales-Pineda, M. (2017). Temperature dependence of apparent respiratory quotients and oxygen penetration depth in contrasting lake sediments. *Journal of Geophysical Research: Biogeosciences*, *122*(11), 3076–3087. https://doi.org/10.1002/2017JG003833

Stefan, H. G., Fang, X., & Eaton, J. G. (2001). Simulated fish habitat changes in North American lakes in response to projected climate warming. *Transactions of the American Fisheries Society*, *130*(3), 459–477. https://doi.org/10.1577/1548-8659(2001)130<0459:sfhcin>2.0.co;2

Tennant, C. J., Harpold, A. A., Lohse, K. A., Godsey, S. E., Crosby, B. T., Larsen, L. G., et al. (2017). Regional sensitivities of seasonal snowpack to elevation, aspect, and vegetation cover in western North America. *Water Resources Research*, *53*(8), 6908–6926. https://doi.org/10.1002/2016wr019374

Terzhevik, A., Golosov, S., Palshin, N., Mitrokhov, A., Zdorovennov, R., Zdorovennova, G., et al. (2009). Some features of the thermal and dissolved oxygen structure in boreal, shallow ice-covered Lake Vendyurskoe, Russia. *Aquatic Ecology*, *43*(3), 617–627. https://doi.org/10.1007/s10452-009-9288-x

Thevenon, F., Adatte, T., Spangenberg, J. E., & Anselmetti, F. S. (2012). Elemental (C/N ratios) and isotopic ($\delta^{15}N_{org}$, $\delta^{13}C_{org}$) compositions of sedimentary organic matter from a high-altitude mountain lake (Meidsee, 2661 m a.s.l., Switzerland): Implications for Lateglacial and Holocene Alpine landscape evolution. *The Holocene*, *22*(10), 1135–1142. https://doi.org/10.1177/0959683612441841

Warne, C. P. K., McCann, K. S., Rooney, N., Cazelles, K., & Guzzo, M. M. (2020). Geography and morphology affect the ice duration dynamics of Northern Hemisphere lakes worldwide. *Geophysical Research Letters*, *47*(12), 1–10. https://doi.org/10.1029/2020GL087953

Woolway, R. I., Kraemer, B. M., Lenters, J. D., Merchant, C. J., O'Reilly, C. M., & Sharma, S. (2020). Global lake responses to climate change. *Nature Reviews Earth & Environment*, *1*(8), 388–403. https://doi.org/10.1038/s43017-020-0067-5

Woolway, R. I., Verburg, P., Lenters, J. D., Merchant, C. J., Hamilton, D. P., Brookes, J., et al. (2018). Geographic and temporal variations in turbulent heat loss from lakes: A global analysis across 45 lakes. *Limnology and Oceanography*, *63*(6), 2436–2449. https://doi.org/10.1002/lno.10950

Zeileis, A., Kleiber, C., Walter, K., & Hornik, K. (2003). Testing and dating of structural changes in practice. *Computational Statistics & Data Analysis*, *44*(1–2), 109–123. https://doi.org/10.1016/S0167-9473(03)00030-6